Incident-photon energy-distribution effects on radiationless resonant Raman scattering

G. Bradley Armen[1] and Honghong Wang[2]
[1]*Department of Physics and Astronomy, University of Tennessee, Knoxville, Tennessee 37996-1200*
[2]*Department of Physics, University of Oregon, Eugene, Oregon 97403*
(Received 25 August 1994)

In the experimental observation of radiationless resonant Raman scattering, features that differ from the idealized case can arise when the spectral width of the incident photon distribution is comparable to the width of pertinent atomic energy levels. These features include nonlinear dispersion of the peak maxima and changes in the symmetry and width of the ejected-electron lines with changes in the average incident photon energy. Under certain conditions, the electron line shapes can become highly asymmetric or even double peaked. The origin of these features in actual experiments is explored through a model calculation for large spectral widths. Some possible applications of these effects are pointed out.

PACS number(s): 32.80.Hd, 32.80.Fb

I. INTRODUCTION

When the energy of monochromatic x rays is tuned just below the threshold for ionization of an atomic inner shell, discrete states can be excited that decay under the ejection of monoenergetic electrons. This process of resonant photon absorption accompanied by electron emission is a form of radiationless resonant Raman scattering (RRRS) ([1–3] and references therein). The scattering process can be envisaged as Auger decay of an ionic core in the presence of a resonantly excited spectator electron, hence the general process has also been referred to as the spectator resonant Auger effect [4] and the RRRS electron lines as spectator Auger lines [5]. What distinguishes RRRS from normal Auger decay is the nature of the intermediate scattering state. Whereas Auger peaks arise when the incident-photon energy is above the ionization threshold, RRRS lines are observed only when the incoming photon's energy is near a specific resonance. There have been many studies of spectator Auger decay following resonant excitation (see, e.g., Refs. [6–9]); however, RRRS is generally associated with specific effects which arise when a *highly* monochromatic source is tuned *across* the resonance: Within this narrow photon-energy range, the position of the RRRS line shifts as the photon energy is changed and the line width is less than that of the corresponding diagram Auger line [10,11]. The RRRS shift is shown [1–3] to be directly proportional to the change in incident-photon energy and observations are interpreted [5,10–15] in this context. However, the RRRS linear dispersion relation holds strictly only for completely monochromatic incident photons. For a given experimental arrangement, the photon-energy spread may not be sufficiently narrow to reflect the expected RRRS behavior in the observed electron spectrum. Since the first observation of RRRS [12], advances in experimental technique and improvements in synchrotron-radiation sources have led to increasingly refined measurements of RRRS. In light of such advances, it is appropriate to investigate some of the finer details that can arise in these types of experiments.

Here we derive a line-shape formula for the ejected spectator Auger electrons, based on a simple, physically intuitive picture. The formula agrees with that derived from scattering theory [1–3,5,15] with certain restrictions. The standard features of RRRS are discussed within the context of this formula, in particular the linear dependence of the RRRS electron-peak position on incident photon energy. The consequences of employing a nonmonochromatic spectral function and an imperfect electron spectrometer are next examined. It is shown that for incident-photon spectral widths comparable to the atomic-state widths the observed spectator Auger features will deviate from the ideal RRRS behavior.

II. THEORY

The RRRS process can be visualized as follows. A beam of incident photons impinges on a sample of atoms. The beam contains photons with a distribution of energies centered on an "average" energy ω_0 (atomic units are used, unless otherwise stated). Individual atoms in the sample, originally in their ground state, absorb photons from the beam and are promoted to an intermediate resonance state. In the present context this intermediate state results from the photoexcitation of an inner-shell electron to a bound unoccupied orbital. This resonance state decays filling the inner-shell vacancy and simultaneously ejecting an electron of energy ε, leaving the residual ion with two vancancies in outer shells. All features of the ejected-electron line shape can be understood intuitively from a statistical model of the photon beam and the atoms of the sample. The process is sketched in Fig. 1 and detailed below.

The incident beam of photons is characterized by a spectral function $G(\omega-\omega_0)$, where ω is the photon energy. The function G is peaked sharply around the "incident energy" ω_0 and represents the probability per unit energy of a given photon having an energy ω.

The statistical character of the target atoms is represented by two distribution functions, one describing the intermediate resonance state, the other describing the

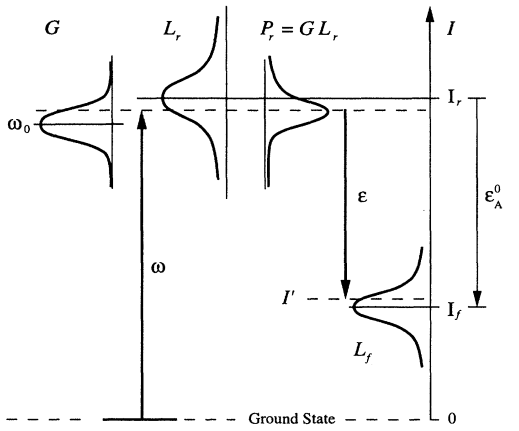

FIG. 1. Representation of radiationless resonant Raman scattering. An incoming beam of photons with the spectral function G selectively excites intermediate states near the resonance energy I_r, resulting in an intermediate-state population P_r. Subsequent spectator Auger decay to the final state results in the ejection of electrons with energies ε, determined by the difference in intermediate and final ionic state energies.

final state of the residual ion after the Auger electron is emitted. An atomic state that decays with a characteristic lifetime τ has an uncertainty $\Gamma = 1/\tau$ in its binding energy. The probability of accessing an atom of the sample in the resonance state with a particular energy I (measured with reference to the ground state) is given by the intermediate resonance-state distribution $L_r(I-I_r)$. This function is sharply peaked around the resonance energy I_r and has a width Γ_r. The (relative) probability of actually exciting a resonance state of energy I is the probability that a photon of energy $\omega = I$ is available and that an atom of the sample can absorb such a photon. The probability (per unit energy) of exciting an intermediate resonance state by the absorption of a photon of energy ω is therefore $P_r(\omega) = G(\omega-\omega_0)L_r(\omega-I_r)$.

The nominal spectator Auger energy is the difference between the binding energies of the resonance and final states $\varepsilon_A^0 = I_r - I_f$. Like the resonance state, the residual ionic state is described by a final-state distribution $L_f(I-I_f)$, which is peaked strongly around the final-state binding energy I_f with a spread Γ_f. The final ionic state can be stable against further decay, in which case $\Gamma_f \to 0$ and $L_f \to \delta(I-I_f)$.

The energy of the atom-plus-photon system is conserved, hence a resonance state of energy I will decay to a final state of energy I' by emitting an Auger electron of energy $\varepsilon = I - I'$. This is indicated in Fig. 1 by the horizontal dashed line of energy $I = \omega$. The probability of ejecting an electron of energy ε from the resonance state with a specific energy I is given by the probability that such an initial state is excited, multiplied by the probability that a final ionic state of energy $I' = I - \varepsilon (= \omega - \varepsilon)$ can be accessed. The total probability of emitting an electron with energy ε is the integral of probabilities over all possible absorption energies

$$P_{\rm em}(\varepsilon) = \int_0^\infty d\omega\, P_r(\omega) L_f(I'-I_f)$$
$$= \int_0^\infty d\omega\, G(\omega-\omega_0) L_r(\omega-I_r) L_f(\omega-\varepsilon-I_f)\,. \quad (1)$$

Apart from factors that describe the probability of excitation and decay relative to all other possible processes [which can be assumed constant over the small energy range in Eq. (1) for which the integrand is nonzero] this line-shape formula is identical to that derived from scattering theory [16] if the resonance is assumed to be isolated and the amplitude for "direct" excitation is negligible. By isolated, it is implied that only one intermediate virtual state contributes significantly to the excitation amplitude, which is expected if the resonance is energetically distant from all others. The resonance and final-state distributions are normalized Lorentz functions centered at I_r and I_f with full widths at half maximum (FWHMs) Γ_r and Γ_f, respectively.

The dependence of the emission line shape on the (average) incident photon energy ω_0 enters in Eq. (1) through the spectral function G. As indicated in Fig. 1, the spectator Auger line shape can, in general, be asymmetric about its maximum owing to asymmetry of the intermediate-state population density P_r. The origin of the RRRS peak shift is suggested in Fig. 1 for the case of below-resonance excitation (a negative relative photon energy $E_{\rm rel} \equiv \omega_0 - I_r$). In this case, P_r is peaked at energies slightly below I_r, hence the spectator Auger line appears on average at slightly lower energies than the nominal ε_A^0. For positive relative energies of excitation, the situation is reversed and the RRRS line moves to energies above ε_A^0.

If the spectral function is very narrow in comparison with the resonance and final states, so that G can be approximated as $G(\omega-\omega_0) = \delta(\omega-\omega_0)$, then we have $P_{\rm em}(\varepsilon) = L_r(\omega_0 - I_r) L_f(\omega_0 - \varepsilon - I_f)$. The *overall* intensity of the RRRS line is determined by the first factor in this expression, which depends on $E_{\rm rel} = \omega_0 - I_r$. For an appreciable signal the photon energy must be near resonance, i.e., $|E_{\rm rel}| \le \Gamma_i$; a maximum signal is produced when $E_{\rm rel} = 0$. For any given ω_0, the electron line shape is determined completely by the final-state function and is thus a Lorentzian of width Γ_f. Since this function is centered at I_f, the maximum of the line occurs at $\varepsilon_{\rm max} = \omega_0 - I_f$. With some of the preceding definitions, this last result can be rearranged to yield the familiar linear-dispersion relation $\Delta_{\rm max} \equiv \varepsilon_{\rm max} - \varepsilon_A^0 = E_{\rm rel}$.

All of these features are characteristic of RRRS: for incident photon energies within a few Γ_r of the resonance energy the RRRS Auger line is shifted from its nominal value by an amount equal to the *relative* photon energy. The emitted RRRS line is narrow [14,15,17], with a width Γ_f. If the final state is stable, or very long lived, then the only limit on the width of the observed electron line shape is instrumental [11]. The total intensity of the line, viewed as a function of incident-photon energy, is a Lorentzian centered on the resonance energy I_r with a width Γ_r. These features are all easily deduced from Fig. 1 by letting the function G, and thus P_r, become "spikes" at the energy ω_0.

Conversely, if the incident-photon distribution is wide in comparison with the initial and final states, as from a "white-light source," the spectral function G can be treated as constant in the convolution (1). In this case, the spectator line shape mimics that of a normal Auger line: a Lorentzian centered at ε_A^0 with a width $\Gamma_r+\Gamma_f$.

For intermediate values of the spectral width, experimental data clearly must display features which are a blend of the two extreme cases, ranging from linear shift to no shift at all. The question of immediate concern is how details of the experimental environment, such as the spectral source and electron spectrometer, modify the RRRS behavior.

In considering the observed line shape, the effect of the electron spectrometer can be included by introducing the "window" function $W(\varepsilon-\varepsilon')$, which describes the probability the spectrometer responds to an electron of energy ε' when set to measure the electron energy ε. In defining W to be a function of electron energy difference only, a number of real-world features are ignored, such as the dependence of source volume and the bandpass on observed electron energy. However, for the small energy ranges involved in measuring a spectator Auger line, the effect of such changes is usually slight. The observed spectator Auger line shape is

$$P_{\rm obs}(\varepsilon)=\int_0^\infty d\varepsilon' W(\varepsilon-\varepsilon')P_{\rm em}(\varepsilon') \ . \tag{2}$$

Averaging by the spectrometer window function causes the emitted line shape to be broadened so that the emitted asymmetry may be washed out. Furthermore, any asymmetry in $P_{\rm em}(\varepsilon)$ will also cause a change in the location of the observed peak maximum [18] due to the averaging properties of the convolution (2). If the asymmetry is slight, however, the observed spectator shift will be very close to that associated with the shape of the emitted line.

The spectator Auger intensity is another important experimental feature. Because the total intensity of the signal is an integral over the entire spectator line, the observed intensity as a function of incident photon energy is proportional to the emitted intensity:

$$\begin{aligned} I_{\rm obs}(\omega_0)&\equiv\int_0^\infty d\varepsilon\, P_{\rm obs}(\varepsilon) \\ &=\left[\int_{-\infty}^\infty dx\ W(x)\right]\left[\int_0^\infty d\varepsilon' P_{\rm em}(\varepsilon')\right] \\ &=wI_{\rm em}(\omega_0) \ , \end{aligned} \tag{3}$$

where w is the overall "efficiency" of the detector [19]. Within the present model, the intensity profile is proportional to the number of final-state ions produced via photoionization (with excitation).

Employing the normalization of the final-state distribution function, integration of Eq. (1) over electron energy yields (for $\varepsilon_A^0 \gg \Gamma_f$) the intensity profile

$$I(\omega_0)=\int_0^\infty d\omega\, G(\omega-\omega_0)L_r(\omega-I_r). \tag{4}$$

The observed intensity profile is simply a convolution of the spectral and resonance-state distributions. These aspects could be of great utility in determining natural widths. In particular, if the spectral width is small, the observed intensity profile (4) will yield the resonance width Γ_r free of instrumental or final-state broadening.

III. RESULTS AND DISCUSSION

To model the incident-photon spectral distribution, the function G is taken to be a normalized Gaussian distribution with a standard deviation σ, or a spectral FWHM of $\Gamma_\omega=2\sigma\sqrt{\ln 4}$. Certainly other choices for the functional form of G may be more appropriate for some experimental situations.

For the purposes of example, we consider the case of Mn K-$L_{2,3}L_{2,3}$ spectator Auger decay in $KMnO_4$. This serves as a good example since the strong atomiclike Mn "$1s\rightarrow 4p$" resonance is well isolated [20]. We make the usual approximation that the presence of the spectator electron does not substantially affect the decay rates of the intermediate or final states. We can then use the Mn diagram K- and $L_{2,3}$-shell vacancy widths [20], setting $\Gamma_r=\Gamma_{1s}=1.16$ eV and $\Gamma_f=\Gamma_{2p,2p}=2\Gamma_{2p}=0.66$ eV.

Equation (1) can be rewritten in terms of the relative photon energy $E_{\rm rel}$ and the relative electron energy $\Delta=\varepsilon-\varepsilon_A^0$:

$$\begin{aligned} P_{\rm em}(\Delta,E_{\rm rel})&=\frac{\Gamma_r\Gamma_f}{(2\pi)^{5/2}\sigma} \\ &\times\int_{-\infty}^\infty dx\frac{e^{-(x-E_{\rm rel})^2/2\sigma^2}}{[x^2+\Gamma_r^2/4][(x-\Delta)^2+\Gamma_f^2/4]} \ , \end{aligned} \tag{5}$$

where the lower integration limit is valid as long as I_r is large in comparison to any of the widths involved. For a fixed value of $E_{\rm rel}$ the integration is performed numerically and features of the line, such as the position of the maximum $\Delta_{\rm max}(E_{\rm rel})$ and the total integrated intensity $I(E_{\rm rel})$ are evaluated.

Figure 2 displays the resulting *emitted* electron line

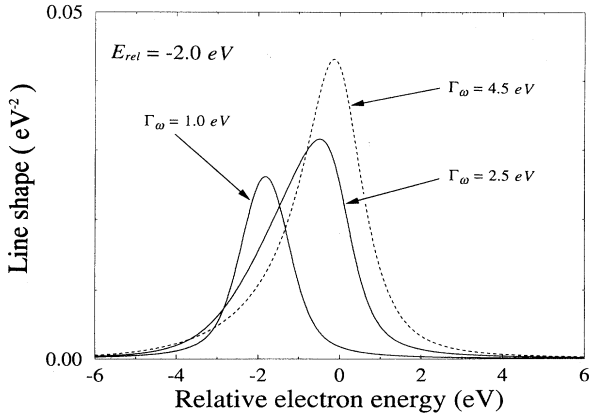

FIG. 2. Emitted spectator Auger line shape when excited with an averge photon energy 2 eV below the resonance state energy ($E_{\rm rel}=-2$ eV). The different lines correspond to different widths (Γ_ω) of the incident photon spectral distribution. The electron energy is measured relative to the nominal spectator Auger energy ε_A^0.

shapes when $E_{rel}=-2$ eV, for three choices of the spectral width ($\Gamma_\omega=1.0$, 2.5, and 4.5 eV). For the choice of $\Gamma_\omega=1.0$ eV, the resulting spectator line shape is a Voigt-like function, with its center shifted from the nominal Auger energy by $\Delta_{max}=-1.82$ eV, and has a spectator FWHM of 1.44 eV. This should be compard with the RRRS line emitted in the limit of small Γ_ω: a Lorentzian centered at $\Delta_{max}=-2.0$ eV with a spectator FWHM of 0.66 eV. Apparently, an experiment employing a spectral width comparable to the natural widths still reflects the basic RRRS features: a peak shift close to the relative photon energy and a line width narrower than the diagram Auger width of $\Gamma_{1s}+2\Gamma_{2p}=1.82$ eV.

As the spectral width is increased, however, the emitted line shape becomes asymmetric and its peak maximum is moved closer to the nominal Auger value. This is illustrated in Fig. 2 by the spectator line shapes resulting when two larger values of Γ_ω are used. The spectator line for $\Gamma_\omega=2.5$ eV is highly asymmetric, with a peak maximum located at $\Delta_{max}=-0.48$ eV. The electron line is also quite wide (2.31 eV FWHM), due to the enhanced low-energy flank.

Finally, when the spectral width is increased further ($\Gamma_\omega=4.5$ eV), the line approaches the "Auger" limit in which the peak maximum is located near ε_A^0 ($\Delta_{max}=-0.13$ eV) and the spectator width (1.83 eV) is close to the diagram Auger width. The line has become more symmetrical and would approach a Lorentz function as Γ_ω is further increased.

The above line shapes were all computed for the case where the average photon energy was 2 eV less than the resonance energy. If E_{rel} is now varied for various fixed spectral widths Γ_ω, the evolution of the electron line shapes can be tracked as the photon source is tuned through the resonance energy. It can be seen from Eq. (5) that $P_{em}(\Delta,E_{rel})=P_{em}(-\Delta,-E_{rel})$, so that all features of the spectator Auger line shape will exhibit symmetry with respect to $E_{rel}=0$. In particular, the relative peak maximum or shift Δ_{max} will be an odd function of E_{rel} and the width of the emitted line and the total line intensity will be even functions of E_{rel}. This is also true in general as long as all the functions of Eq. (1) are symmetric about their centers.

Figure 3 displays the same three spectator Auger peaks, but now excited with an average photon energy 5.5 eV greater than the resonance energy ($E_{rel}=+5.5$ eV). It is seen that some dramatic changes from the $E_{rel}=-2$ eV example of Fig. 2 have occurred. Since these peaks are the result of excitation much farther from resonance, their overall intensities are reduced from those in Fig. 2. The peak excited with the narrowest spectral function ($\Gamma_\omega=1.0$ eV) still exhibits near-ideal RRRS behavior with a peak shift $\Delta_{max}=5.43$ eV and its width of 1.40 eV is little changed from Fig. 1. The peak corresponding to $\Gamma_\omega=2.5$ eV has now become symmetric, but its width has increased to 2.99 eV. Finally, the peak resulting from excitation with the largest spectral width ($\Gamma_\omega=4.5$ eV) has become very broad (6.71 eV) and has developed two distinct maxima.

Figures 2 and 3 indicate that the evolution of the spectator Auger line shape can be quite complicated as the incident photon energy and spectral width are varied. It is instructive to examine how the gross features of the line shape behave as a function of E_{rel}.

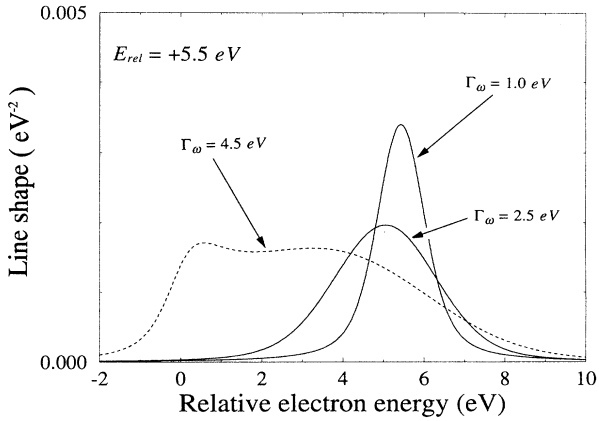

FIG. 3. Emitted spectator Auger line shape when excited with an average photon energy 5.5 eV above the resonance energy. The results for three spectral widths are indicated.

Figure 4 shows a plot of the widths of the emitted electron lines as a function of the relative photon energy E_{rel}, again for the three choices of incident spectral width Γ_ω. The lower horizontal dashed line indicates the RRRS limit ($\Gamma_\omega=0$) where the emitted electron line width takes on the final-state width of 0.66 eV, independent of E_{rel}. The upper horizontal dashed line indicates the white-light limit of 1.82 eV. It is seen that for all three cases of finite spectral width, there is a dependence of the emitted line-shape widths on E_{rel} and the lines are narrowest at resonance. In the case of $\Gamma_\omega=1.0$ eV, the line width is still narrow, with only a slight dip near resonance, but for larger spectral widths the variation with E_{rel} becomes more pronounced.

Numerical experimentation indicates a rough correla-

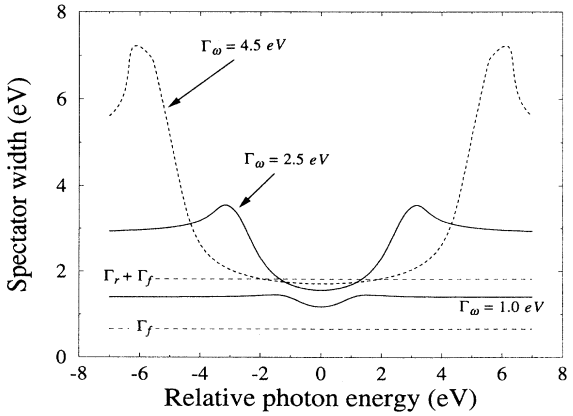

FIG. 4. Widths of the spectator Auger electron line shapes, as a function of the relative photon energy $E_{rel}=\omega_0-I_r$, for three incident spectral widths. The dashed horizonal lines indicate the RRRS (lower) and the white-light (upper) limits.

tion betwen the asymmetry of the spectator peak and the *derivative* of the spectator-width curves of Fig. 4. That is, for regions of E_{rel} in which the spectator width changes most rapidly, the peaks are found to be most asymmetric. Also, the "direction" of the asymmetry is correlated to the sign of the change. For example, consider the $\Gamma_\omega=2.5$ eV case in Fig. 4 and the slope of this curve at various values of E_{rel}. At resonance ($E_{rel}=0$ eV) the line is narrow and completely symmetric. Moving to excitation above resonance, the Auger line-shape asymmetry and width grow, the line developing an enhanced *high*-energy shoulder. Maximum asymmetry occurs at about $E_{rel}=2.4$ eV and then decreases unitl the line again becomes symmetric, very near $E_{rel}=3.0$ eV where the maximum width occurs. Further increasing E_{rel}, the spectator line develops an enhanced *low*-energy shoulder and reaches a maximum (reverse or negative) asymmetry near $E_{rel}=3.3$ eV. Beyond this point, the line shape becomes more symmetric.

Above or below resonance, the same general interpretation of the slope can be employed: positive slope is connected with "positive" line-shape asymmetry (an enhanced high-energy shoulder to the peak) and negative slope with "negative" asymmetry (a low-energy shoulder).

For the case of large spectral width $\Gamma_\omega=4.5$ eV, the high-energy shoulder evolves into a separate peak as E_{rel} is increased from zero and the above guidelines are less applicable; still the general trend is the same. For $5.4 \le E_{rel} \le 5.9$ eV two clearly discernible maxima coexist. Within this region of E_{rel}, dominance shifts from the low-energy maximum to the high-energy maximum. Above $E_{rel}=6.0$ eV the low-energy peak disappears, becoming a low-energy shoulder, which gradually subsides as E_{rel} is increased further.

The shifts of the spectator peak maxima away from ε_A^0 are displayed as a function of E_{rel} in Fig. 5. For $\Gamma_\omega=1.0$ eV, it is seen that the spectator shift deviates only slightly from the linear dispersion expected for zero spectral width. Larger deviations occur when the spectral distribution is widened; Fig. 5 also displays the shifts for the cases $\Gamma_\omega=2.5$ and 4.5 eV. It is seen that as the spectral width is increased, the shift becomes flattened in the photon energy range over which the peak can be observed, approaching the white-light limit of no shift.

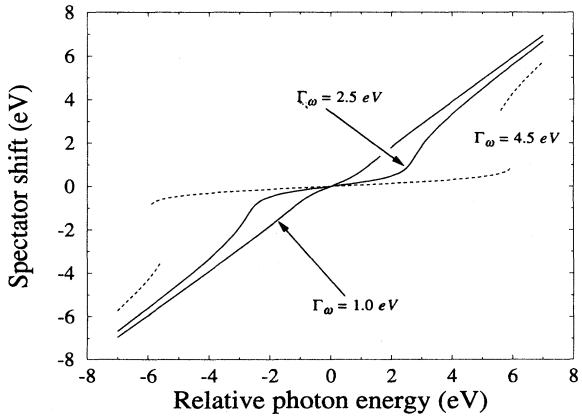

FIG. 5. Plot of the spectator Auger shift $\Delta_{max}=\varepsilon_{max}-\varepsilon_A^0$ relative to the nominal spectator Auger energy ε_A^0, as a function of the relative photon energy. The results for three spectral widths are indicated. For the case of $\Gamma_\omega=4.5$ eV, the line shape develops two maxima for average photon energies in the ranges $5.5<|E_{rel}|<6.0$ eV.

For the cases such as the $\Gamma_\omega=2.5$ eV example of Fig. 5, the nonlinear spectator dispersion may be noticeable as systematic deviations away from a fit of peak maxima to the linear model. This may provide a partial explanation of such small deviations in recent InP data [Ref. [15], Fig. 6(c)]; however, the analysis is complicated by the possible presence of unresolved multiplet splitting or even several resonances.

In the large spectral width case ($\Gamma_\omega=4.5$ eV), the emergence of two maxima is visible in Fig. 5 as regions of E_{rel} where the dispersion curve becomes double valued. The discontinuities in the dispersion curve reflect the rapid transfer of intensity from the low-energy to the high-energy peak as E_{rel} is increased within these regions.

The emergence of two maxima in the spectator line shape, when the spectral function is sufficiently broad and $E_{rel} \approx \Gamma_\omega + \Gamma_r$, can be understood from Fig. 1. Under these conditions, the intermediate-state population density P_r acquires two maxima. This is because the flank of the spectral function G provides a roughly constant multiplier near the resonance-distribution center and the broad wings of the Lorentzian resonance act similarly near the center of G. In general, the conditions for this splitting are restrictive and depend critically on the shape of the spectral function. For the case of a negligible final-state width, Gel'mukhanov and Ågren [21] have derived such conditions for several forms of the spectral function. Some indication of this kind of splitting can be seen in calculations of the radiative Raman scattering process [22].

The above results for the spectator line shapes, shifts, and widths must be further modified by the spectrometer averaging of Eq. (2). Although we do not pursue this issue, a few additional remarks can be made. Because the spectator Auger line shapes can become quite asymmetric, the window averaging has the potential to change the location of the peak maximum relative to that of the emitted maximum. This additional shift will be in the direction of the asymmetry, e.g., an asymmetric peak with a high-energy flank will, upon averaging by a symmetric window function, become less asymmetric and wider with a maximum shifted to higher energy.

The remaining experimental feature to discuss is the intensity profile of Eq. (4). This is the (integrated) spectator Auger intensity, viewed as a function of average incident-photon energy. It is obvious from Fig. 1 that the intensity of the emitted line will be a maximum when the averge photon energy is equal to the resonance energy ($E_{rel}=0$). It is also clear that the broader the spectral function, the larger the range of photon energies over which the spectator Auger line can be observed. In the limit of vanishing spectral width the intensity profile becomes a Lorentz function of FWHM Γ_r. This property can be taken as a guide in defining the *observation width*

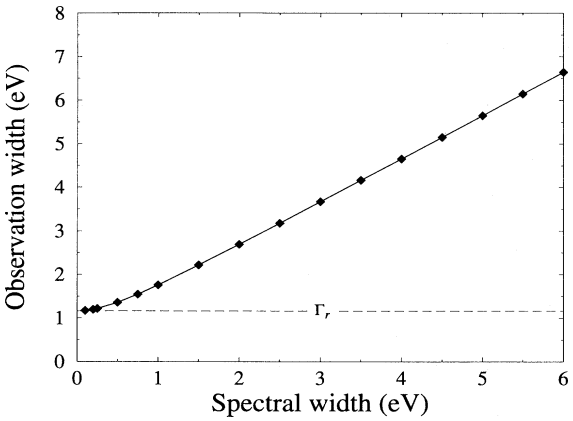

FIG. 6. Plot of the observation width, the range of excitation energies over which a spectator Auger can be observed with "reasonable" intensity, versus the incident-photon spectral width. The diamonds indicate calculated values, which are connected by straight lines.

to be the FWHM of the intensity profile, that is, the tunable range of incident-photon energy over which the integrated intensity is greater than one-half the intensity at resonance. In Fig. 6 the observation width is plotted as a function of the spectral FWHM Γ_ω for the present example.

In the present case, Eq. (4) reduces to the convolution of a Gaussian and a Lorentzian function. The intensity profile is therefore a Voigt function and the observation range is the FWHM of this function. As long as the approximations discussed in connection with Eqs. (2) and (3) are valid, the results of Fig. 6 are independent of the electron spectrometer used. Additionally, it is completely independent of any details concerning the final state. A measurement of the observation width for a known spectral function could therefore be employed to extract the resonance width. Several measurements of the intensity profile using different spectral widths could be employed for consistency.

Because the spectator shift vanishes at zero relative photon energy and departures from linear dispersion are antisymmetric about $E_{\rm rel}=0$, it might be argued that employing a purposely wide but accurately known spectral distribution would be of advantage: If the spectral function were known along with the resonance and final-state widths, a fit of the dispersion function $\Delta_{\max}(E_{\rm rel})$ could reveal both the resonance energy and nominal spectator Auger energy, and hence the final-state binding energy. Because the location of peak maxima can in general be determined to better accuracy than line intensity, a fit of data directly to the dispersion curve has the potential for greater accuracy in determining I_r than a fit for the intensity-profile center. Conversely, if the experimental parameters and energies were well known, information regarding the natural widths of the intermediate and final states could be extracted. A series of such experiments, repeated for different values of the incident-photon spectral width, could provide sufficient data to extrapolate the electron line shapes and the intensity profiles, to the pure RRRS regime (zero spectral width), yielding Γ_f and Γ_r, respectively.

It must be stressed that the physics of RRRS lies in the transition matrix, in the present context the limit of a monochromatic source and a perfect electron spectrometer. The essence of RRRS is a linear dispersion relation for the peak shifts and a RRRS electron line shape that only reflects the width of the final ionic state. The plethora of new features outlined above are not the result of new physics, but simply the observational consequence of a particular averaging of RRRS features, dictated by a given experimental setup.

IV. CONCLUSION

In conclusion, we have presented a statistical model of the RRRS process, which is helpful in visualizing the scattering experiment. Because this model depends only on the most fundamental consequences of the existence of a resonance, it is equally applicable to RRRS in atoms, molecules, or solids. This intuitive picture will need modification if there are a number or resonance states which lie close in energy. We have explored the experimental features to be expected when the spectral distribution of incident light is wide. These features include nonlinear dispersion of the peak maxima and variation of the symmetry and the width of the spectator Auger lines with average photon energy. Under certain conditions, the electron line shapes can be highly asymmetric and even develop a double-peak structure.

ACKNOWLEDGMENTS

We thank T. Åberg and B. Crasemann for many useful comments on the manuscript and H. Ågren for communication of work performed prior to publication. This work has been supported by the National Science Foundation.

[1] T. Åberg and B. Crasemann, in *Resonant Anomalous X-Ray Scattering: Theory and Applications,* edited by G. Materlik, C. J. Sparks, and K. Fischer (North-Holland, Amsterdam, 1994), p. 431.

[2] B. Crasemann, Comments At. Mol. Phys. **22**, 163 (1989).

[3] T. Åberg, Phys. Scr. **T41**, 71 (1992).

[4] F. P. Larkins, J. Electron Spectrosc. Relat. Phenom. **51**, 115 (1990).

[5] G. B. Arman, T. Åberg, J. C. Levin, B. Crasemann, M. H. Chen, G. E. Ice, and G. S. Brown, Phys. Rev. Lett. **54**,

1142 (1985).
[6] C. D. Caldwell, M. G. Flemming, M. O. Krause, P. van der Meulen, C. Pan, and A. F. Starace, Rev. A **41**, 3401 (1989).
[7] H. Aksela, S. Aksela, J. Tulkki, T. Åberg, G. M. Bancroft, and K. H. Tan, Phys. Rev. A **39**, 542 (1990).
[8] T. Hayaishi, A. Yagishita, E. Murakami, E. Shigemasa, Y. Morioka, and T. Sasaki, J. Phys. B **23**, 1633 (1990).
[9] S. B. Whitfield, J. Tulkki, and T. Åberg, Phys. Rev. A **44**, R6983 (1991).
[10] A. Kivimäki, A. Naves de Brito, S. Aksela, H. Aksela, O.-P. Sairanen, A. Ausmees, S. J. Osborne, L. B. Dantas, and S. Svensson, Phys. Rev. Lett. **71**, 4307 (1993).
[11] H. Aksela, S. Aksela, O.-P. Sairanen, A. Kivimäki, A. Naves de Brito, E. Nõmmiste, J. Tulkki, S. Svensson, A. Ausmees, and S. J. Osborne, Phys. Rev. A **49**, R4269 (1994).
[12] G. S. Brown, M. H. Chen, B. Crasemann, and G. E. Ice, Phys. Rev. Lett. **45**, 1937 (1980).
[13] G. E. Ice, G. S. Brown, G. B. Armen, M. H. Chen, B. Crasemann, J. Levin, and D. Mitchell, in *X-Ray and Atomic Inner-Shell Physics,* edited by B. Crasemann, AIP Conf. Proc. No. 94 (AIP, New York, 1982), p. 105.
[14] W. Drube, A. Lessmann, and G. Materlik, in *Resonant Anomalous X-Ray Scattering: Theory and Applications* (Ref. [1]), p. 473.
[15] H. Wang, J. C. Woicik, T. Åberg, M. H. Chen, A. Herrera-Gomez, T. Kendelewicz, Anna Mäntykenttä, K. E. Miyano, S. Southworth, and B. Crasemann, Phys. Rev. A **50**, 1359 (1994).
[16] See, e.g., the discussions relating to Eq. (15) of Ref. [11], or to Eqs. (1)–(3) of Ref. [5].
[17] T. LeBrun, S. H. Southworth, M. A. MacDonald, and Y. Azuma (unpublished).
[18] J. Tulkki, G. B. Armen, T. Åberg, B. Crasemann, and M. H. Chen, Z. Phys. D **5**, 241 (1987). Figure 3 illustrates the additional shift resulting from the convolution of an antisymmetric peak with a symmetric one.
[19] The factorization in Eq. (3) is possible so long as ε_A^0 is large in comparison to the width of the spectrometer window function, permitting the lower integration limit to be effectively set to $-\infty$.
[20] J. Tulkki and T. Åberg, J. Phys. B **15**, L435 (1982), and references therein.
[21] F. Gel'mukhanov and H. Ågren, Phys. Lett. A (to be published).
[22] T. Åberg and J. Tulkki, in *Atomic Inner-Shell Physics,* edited by B. Crasemann (Plenum, New York, 1985), p. 419.